# INVESTIGATION OF FLAME STRUCTURE OF HMX/GAP PROPELLANT AT 0.5 MPa*

**O.P. Korobeinichev, A.A. Paletsky, E.N. Volkov, A.G. Tereschenko, and P.D. Polyakov**
Institute of Chemical Kinetics and Combustion, RAS Siberian Branch, 630090 Novosibirsk, Russia

## ABSTRACT

The chemical and thermal structure of HMX/GAP propellant flames was investigated at a pressure of 0.5 MPa using molecular-beam mass spectrometry and a microthermocouple technique. The pressure dependence of the burning rate was measured in the pressure range of 0.5 – 2 MPa. A probing method for flame sampling that allows for the detection of products of propellant decomposition (including HMX vapor) in the zone adjacent to the burning surface was developed. Eleven species, including HMX vapor, were detected in a zone adjacent to the burning surface. Species concentrations were determined at different distances from the burning surface. Temperature profiles in the combustion wave were measured. Two zones of chemical reactions in the flame were found. It has been found that the composition of combustion products and the temperature of HMX/GAP propellant at 0.5 MPa are close to those at thermodynamic equilibrium. Data obtained can be used for creation and validation of combustion models for propellants based on HMX and GAP.

* Key Words: HMX, GAP, nitramine propellant, flame structure, high pressure

## 1. INTRODUCTION

Studies of the combustion mechanism of composite propellants (CP) based on cyclic nitramine (HMX) with glycidyl azide polymer (GAP) as an active binder are of both practical and theoretical interest. Practical interest is motivated by the use of high energetic materials (EMs) in solid propellants (SP), which provide good ballistic characteristics to propellants. At the same time, progress in the development of a model of propellant combustion strongly depends on the understanding of SP combustion mechanism and availability of combustion models for individual propellant ingredients (mainly oxidizers) based on realistic physicochemical processes and detailed kinetic mechanism of reactions in flame. The combustion mechanisms of HMX and GAP have been studied extensively. Therefore an HMX/GAP propellant is also a good subject for investigation of SP combustion mechanisms. Investigation of combustion chemistry and flame structure of this propellant can make an important contribution to the creation of its combustion model. The thermal structure of the self-sustained combustion wave of HMX/GAP propellant over a wide pressure range has been thoroughly investigated using a microthermocouple technique [1, 2]. The chemical structure of the HMX/GAP flame in laser-assisted combustion at atmospheric pressure was investigated using microprobe mass spectrometry in [3]. A model for HMX/GAP combustion was created [4]. A comparison of calculated results of [4] with experimental data on the flame structure of laser-assisted combustion [3] showed that they are in fairly good agreement. It was shown earlier that in laser-assisted and self-sustained combustion, some EMs (RDX, HMX) have different flame structures. Thus, it is not possible to model self-sustained combustion using the results obtained for laser-assisted combustion. However, there are no experimental data on the chemical structure of flame for the self-sustained combustion of HMX/GAP propellant at high pressures (0.5 MPa and higher). The goal of the present paper is to make up for this deficiency. Such data are needed to create a model for the self-sustained combustion of this propellant.

## 2. EXPERIMENTAL

The HMX/GAP (80/20 wt%) flame structure at pressure of 0.5 MPa was investigated using a molecular beam probe mass spectrometry (MBPMS) method described in [5], a microthermocouple technique, and video recording. In MBPMS of EM flames, the burning strand moves toward the probe at a rate exceeding the propellant burning rate.

GAP was synthesized and certified at the St. Petersburg Technological University. Some physico-chemical characteristics of HMX/GAP propellant and its ingredients are presented in Table 1.

**Table 1**
Physico-chemical properties of the propellant and its ingredients

| | GAP | HMX |
|---|---|---|
| Name | Glycidyl azide polymer | Cyclotetramethylene tetranitramine |
| Formula | Monomer - $C_3H_5N_3O$<br>Brutto - $C_{60}H_{104}O_{21}N_{54}$<br>Number of hydroxyl groups - 2.58 | $C_4H_8N_8O_8$ |
| Molecular weight, g/mole | 1970 (average) | 296 |
| Density, g/cm$^3$ | 1.275 | 1.9 |
| Enthalpy of formation, kcal/kg | 146 | 71 [6] |
| Brutto-formula of HMX/GAP (80/20 wt%) propellant | $C_{17.1}H_{32.5}N_{27.2}O_{23.8}$ | |
| Enthalpy of formation of the propellant, kcal/kg | 86 | |
| Density of the propellant, g/cm$^3$ | 1.69±0.01 | |

Propellant samples were prepared by mixing HMX powder (a bimodal mixture of crystals with a coarse fraction with particle size of 150-250 μm and a fine fraction with particle size less than 20 or 50 μm in a 50/50 wt% ratio) and GAP (yellow viscous liquid). The mixture was prepared in dry air and was then evacuated before sample preparation. The sample density was equal to 1.69±0.01 g/cm$^3$ (~98% of the calculated density).

Experiments on combustion of uncured HMX/GAP propellants at pressures of 0.5-2 MPa were conducted in a high-pressure combustion chamber in an atmosphere of nitrogen or argon. The burning rates, which are known to depend on pressure, were determined by visualization of the motion of the propellant burning surface using video recording.

The thermal structure of uncured HMX/GAP propellant flame at 0.5 MPa was investigated using ribbon WRe(5%)-WRe(20%) thermocouples embedded in the sample. The thermocouples were made by rolling wires with a diameter of 50 μm. The thermocouples had a thickness (h) of 15 μm. Arms of the thermocouples were bent at right angle at a distance of 100h from the thermocouple's junction. The resulting shape of the thermocouple looks like Greek letter "Pi". The length of the thermocouple shoulders (l) was equal to 3.0 mm, i.e. the ratio l/h in our experiment was equal to 200. At such a ratio, the temperature measurement error due to heat losses in thermocouple shoulders does not exceed 2% [7]. A method for embedding of the microthermocouple in viscous propellant mixture was developed. In order to prevent flame propagation along the side surface, the samples were placed in cylinders made of thin cigarette paper treated with an aqueous solution of ammonium perchlorate. This enabled the propellant to burn evenly, and did not prevent observation of the burning surface.

With the use of Pt-PtRh(10%) thermocouples with a diameter of 20 μm, it was not possible to obtain useful results. This was most likely the result of overheating due to catalytic recombination of radicals, which led to destruction of thermocouples. The strand was ignited by an electrically heated nichrome wire of special shape, which was placed at 0.5-1 mm above the sample surface. Preliminary experiments demonstrated the final temperature of combustion products of HMX/GAP propellant to be about 2100 °C. At such a temperature probing of the flame can be carried out using an aluminum probe covered by $Al_2O_3$. However, in the near-surface zone, at a temperature of 400-500 °C, a "cold" aluminum probe can lead to condensation of HMX vapor inside the probe's orifice, thereby making its identification impossible. Therefore the investigation of flame structure of the HMX/GAP propellant was conducted using quartz probes. Quartz "sonic" probes with different wall thickness (Δr) and with an orifice diameter of 30-40 μm were used for sampling. The opening angle of the internal cone of the probes was equal to ~ 40°. Three types of probes were used: a thick-walled (Δr=1.4 mm) probe with additional heating similar to that described in [8] (Probe 1); a thick-walled probe with wall thickness near the probe orifice less than in Probe 1 (Δr=0.35 mm) without additional heating (Probe 2); and a thin-walled probe (Δr=0.17 mm) without additional heating (Probe 3). The main goal of using the probe with additional heating was to increase the temperature of the probe tip to a value slightly higher than the temperature of the propellant burning surface (330 °C [2]). This prevented plugging of the probe orifice due to HMX vapor condensation on the inner walls of the probe near its tip. At the same time, this allowed detection of HMX vapor in the low-temperature flame zone near the burning surface. At first, preliminary experiments on burning of samples with different dimensions at a pressure of 0.5 MPa were conducted. These experiments allowed us to determine the maximum time of sampling from HMX/GAP flame during which fusion of the orifice of the probe or failure of the probe did not occur. The height of samples varied from 2 to 4 mm, and the diameter - from 3 to 8 mm. Experiments showed that quartz probes of different types became unfit, on average, after four or five experiments. In the case of Probes 1 and 2, failure of the probe orifice occurred if the residence time of the probe in flame exceeded 2 s. For Probe 3, the residence time of the probe in the flame should not exceed 0.6 s. Conditions of experiments for determination of flame structure (rate of sample movement toward the probe, initial distance between sample and the probe) were defined on the basis of the results of the preliminary experiments described above.

To obtain quantitative composition of combustion products, the mass spectra of individual species $H_2$, $H_2O$, HCN, $N_2$, CO, NO, $CH_2O$, $N_2O$, $NO_2$, $CO_2$ and HMX vapor ($HMX_v$) were obtained, and their calibration coefficients $k_{i/Ar}$ measured. The calibration coefficient is defined as $k_{i/Ar} = \Delta I_{Ar} P_i / I_i P_{Ar}$, where $I_{Ar}$ and $I_i$ are

the intensities of argon and *i* species peaks, respectively; and $P_{Ar}$ and $P_i$ are the corresponding partial pressures in the combustion chamber or in the reactor. The mole fraction in our experiments was defined as

$$\alpha_i = I_i k_{i/Ar} / (\Sigma I_j k_{j/Ar}),$$

where $I_i = I_{i(exp)} - \Sigma I_{j(i)}$; $I_i$ is the mass peak intensity of *i* species; $I_{i(exp)}$ is the initial experimental intensity; and $\Sigma I_{j(i)}$ is the sum of intensities of all *j* species (except *i* species), which make contributions into $I_{i(exp)}$. Calibration of the MBPMS for species was conducted in a flow reactor at constant pressure in a pressure range of 0.3 – 0.4 MPa. Calibration gas (10-50% of total volume flow) was introduced in the flow reactor in a mixture with the carrier gas. Calibrations were conducted with a gas temperature of ~ 300-350 °C and the same temperature of the tip of the probe. The experimental temperature of the final combustion products (T=2550 K) was very close to the calculated temperature at thermodynamic equilibrium (T=2555 K). Therefore, the composition of the final combustion products should be very close to the calculated composition at thermodynamic equilibrium. With this assumption, the calibration coefficients for the final combustion products ($H_2$, $H_2O$, $N_2$, CO and $CO_2$) were determined using measured intensities of mass peaks (2, 14, 18, 22, 28 and 44) and the calculated composition at thermodynamic equilibrium. Comparison of the thus obtained calibration coefficients with results of direct measurements showed that they coincide with good accuracy (except for $CO_2$). It was difficult to obtain a correct experimental calibration coefficient for $CO_2$ because this gas readily forms clusters during expansion in the probe nozzle. The calculated coefficients (for $H_2$, $H_2O$, $N_2$, CO and $CO_2$) and measured coefficients for other species were used to determine the combustion product composition near the burning surface. To identify HMX vapor, we performed special experiments on HMX evaporation in the flow reactor (Fig.1) (quartz tube 10 mm in diameter) using the MBPMS setup and Probe 1. This technique was described in detail elsewhere [9]. The experiments were performed at atmospheric pressure in the flow of 0.8-1.5 $cm^3/s$ of argon or nitrogen. Drops of an HMX solution in acetone were applied on the central part of the heater. As acetone evaporates, HMX crystals with sizes less than 0.04 mm formed on the heater surface. The sample weight was less than 1 mg. The heater includes a tungsten plate 0.1 mm thick and 1 mm wide that is placed inside the tube at a distance of 2 mm from the probe's orifice. The carrier gas was fed through this same tube. The temperature of the probe tip was 300 °C, as in the experiments with flame probing. The plate was heated by an electric current at a heating rate of 700 K/s up to the melting point of HMX (280 °C) and then at a heating rate about 75 K/s thereafter. The temperature of the plate was measured by a chromel-alumel thermocouple that was 0.03 mm in diameter and welded to the backside of the plate directly opposite the HMX sample position.

It should be specially noted that the largest difficulties were caused by calibration of the molecular beam sampling system for HMX vapor under conditions of high pressure. Earlier, the vapor of HMX was observed under vacuum in HMX decomposition in a Knudsen cell at a pressure of ~ $10^{-2}$ Torr [10]. HMX vapor was observed during the rapid decomposition of a small samples of HMX (less than 1 mg) in a flow reactor at 0.1 MPa [11]. Optimum experimental conditions to obtain HMX vapor for calibration were chosen based on studies of the behavior of HMX samples at the heating on the plate in the flow reactor using video recording. Heating rate, maximum temperature, flow rate and even construction of the plate were varied. At low flow rates and a temperature in the center of the plate of ~ 300 °C, we observed the melting of a sample placed in the center of plate and the formation of a large quantity of long crystals with diameter of 20 – 30 μm on colder ends of plate. The crystals were formed as a result of the condensation of

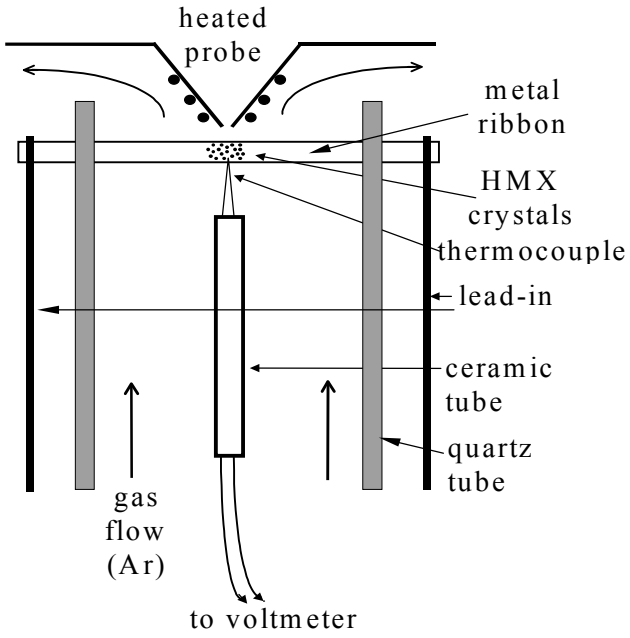


**Figure 1**. Flow reactor for HMX thermal decomposition at 0.1 MPa.

HMX vapor from the gas phase. It proves the fact that the HMX sample had vaporized. It was necessary to meet a number of experimental requirements in order to provide a concentration of HMX vapor such that it prevailed over that of HMX decomposition products. These requirements consist of:

1. A small size of the initial crystals, which melt under heating producing the drops. When the crystal size decreases, the fraction that evaporates increases. In addition, the possibility of overheating of the drops decreases. This is important, because overheating can lead to explosion.
2. A sufficiently high velocity of the carrier gas and a short distance between the heated sample and the probe orifice are needed to provide the rapid transfer of vapor to the probe and prevent condensation.
3. The tip of the probe must be heated up to a high enough temperature to prevent HMX vapor from condensing on the walls near the probe orifice.

In HMX calibration, as the mass peak intensities of HMX vapor ($\Delta I_{HMX}$) increase, the mass peak intensities of the carrier gas decrease ($\Delta I_{Ar}$). For HMX vapor, the calibration coefficient was determined from the formula: $K_{HMX/Ar} = \Delta I(42)_{HMX}/\Delta I(40)_{Ar}$, where I(42) is the intensity of mass peak 42, which is the largest peak in the mass spectrum of HMX.

## 3. RESULTS AND DISCUSSIONS

### 3.1. Burning rate

Burning rate versus pressure relationships for pure HMX and uncured HMX/GAP propellants (formulated with bimodal HMX) obtained by different investigators (Kubota [1] and Zenin [2]), including our data, are presented in Fig. 2. Table 2 shows that there are differences between propellant compositions used. The fine fraction of HMX was less than 20 μm in our experiments and less than 50 μm in [2]. The burning rates of pure HMX over the pressure range of 0.5-2 MPa are higher than those of HMX-based propellants with active binder GAP. The pressure dependence of the burning rate for the propellant investigated in the pressure range of 0.5-2.0 MPa can be presented as $r_b=1.6\times P^{0.78}$, where $r_b$ is the burning rate (in mm/s) and P is the pressure (in MPa). Burning rates of propellants used in [2] (with fine fraction of HMX <50 μm) and in our work (with fine fraction <20 μm) are close to each other at 1.0 and 2.0 MPa, but differ by 1.5 times at pressure of 0.5 MPa.

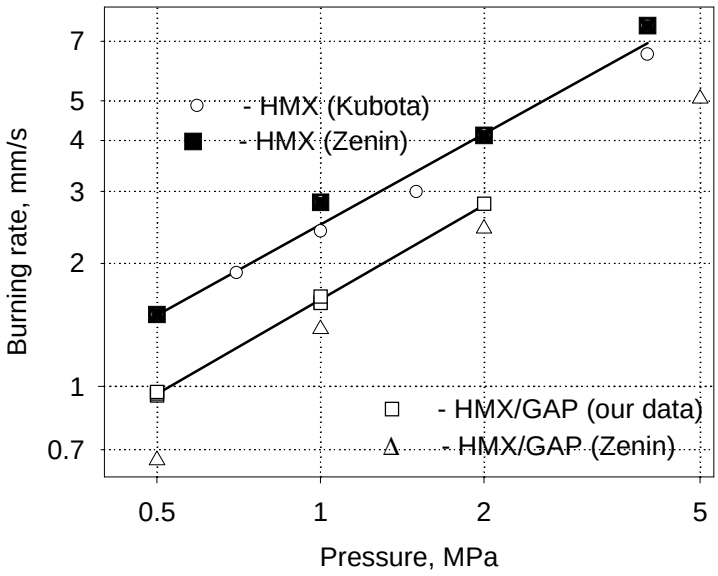


**Figure 2.** Pressure dependence of burning rate of HMX/GAP propellant (uncured) (80/20 wt%) and of pure HMX.

**Table 2**
Elemental composition of uncured propellant HMX/GAP (80/20 wt%)

| | C | H | N | O |
|---|---|---|---|---|
| Our data | 17.1 | 32.5 | 27.2 | 23.8 |
| Litzinger et al. [3] | 16.9 | 31.7 | 27.7 | 23.7 |
| Zenin et al. [2] | 17.896 | 21.811 | 26.886 | 24.156 |

### 3.2. Temperature measurements

In Fig.3, temperature profiles (two profiles for each propellant) in the flame of HMX/GAP (80/20) propellant with different particle size of the fine fraction, and at 0.5 MPa are presented. Mass of fine fraction comprises 50 wt% of total mass of nitramine in the propellant. Replacement of HMX with particles size of ≤20 μm ($HMX_{20}$/GAP propellant) by a fraction with particle size of ≤50 μm ($HMX_{50}$/GAP propellant) did not change the temperature gradient near the burning surface up to a distance of 0.05 mm (it corresponds to the temperature of ~ 500 °C), but resulted in a significant changes in the temperature profile at distances >0.05 mm (Fig 3). A comparison of the data obtained in [2] and in the present study shows that a change in the trend of the temperature curve is observed at a temperature of ~ 1000 °C. In the case of $HMX_{50}$/GAP propellant this temperature is achieved at a distance of ~ 0.4 mm from the burning surface, whereas in the case of $HMX_{20}$/GAP this distance is 2 times less. The maximum temperature for $HMX_{50}$/GAP propellant at 0.5 MPa is equal to ~ 2200 °C and is achieved at a distance of 0.8-0.9 mm. For $HMX_{20}$/GAP propellant the same temperature was measured at a slightly larger distance (~ 1.1 mm). It is noteworthy that the composition of uncured $HMX_{50}$/GAP (80/20 wt%) propellant, investigated in our work, coincides with the composition of propellant investigated in [2]. But temperature profiles do not coincide with each other. Results of our investigation significantly differ from data [2] by the width of the flame zone and by value of the maximum temperature, corresponding to the final products. The maximum temperature was achieved in [2] at a distance of 1.6 mm and was equal to 1900 °C. The possible reason for the difference between our data and data in [2] obviously relates to a difference in GAP (elemental composition, enthalpy of formation) and the density of the propellant. The density of the propellant used in [2] was 88% of the theoretical maximum density (TMD) versus ~98% in our case.

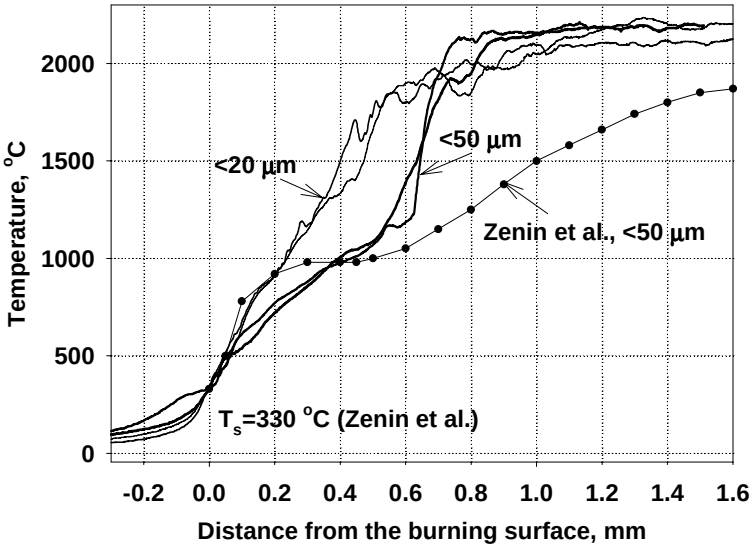


**Figure 3.** The influence of particle size of fine fraction of HMX on temperature profile in the combustion wave of HMX/GAP propellant at 0.5 MPa.

The main difference in experimental data for HMX/GAP propellant at 0.5 MPa that has not yet been explained is the existence of extensive (~ 0.3 mm) region in the temperature profile (at temperature of ~ 1000 °C) according to [2] and absence of it in our experiments.

### 3.3. Combustion product composition of HMX/GAP propellant at 0.5 MPa

Investigation of flame structure of uncured composite $HMX_{20}$/GAP (80/20) propellant was conducted at 0.5 MPa in an atmosphere of argon using quartz Probe 1, 2 and 3. Propellant samples having a length of ~ 2 mm and diameter of 4-8 mm were used in the investigation. An analysis of samples taken from the flame identified the main species in the flame: $H_2$ (2), $H_2O$ (18, 17), HCN (27, 26, 14), CO (28, 12), $N_2$ (28, 14), $CH_2O$ (29, 30), NO (30, 14), $CO_2$ (44, 22), $N_2O$ (44, 30, 28, 14), $NO_2$ (46, 30, 14), and $HMX_v$ (75, 46, 42, 30, 29). The mass peaks used to identify species and determine their concentrations are shown in parentheses. Results of typical measurements are presented in Fig. 4. Differentiation of species with the same mass-to-charge ratio was performed using mass spectra of individual species as obtained from calibration experiments. Relative contributions of $CO_2$ and $N_2O$ to mass peak 44 were determined in the whole flame zone by using mass peak 22 ($CO_2^{++}$). Contributions of $N_2$ and CO into mass peak 28 were

determined only in the final flame zone (at the distance of ~1 mm from the burning surface) using intensity of mass peak 14 ($N^+$), because there are no other nitrogen-containing products. Near the burning surface, CO and $N_2$ could not be distinguished from each other because of the large intensity of mass peaks 30, 44, 27 from the intermediate products NO, $N_2O$, HCN and their significant contribution to mass peak 14 in this zone.

The location of the burning surface was determined by noting an abrupt change in the majority of mass peak intensities (Fig.4) that occurs at the moment the probe touches the liquid layer on the propellant surface. For example, in Figure 4, the data points collected at what was determined to be the burning surface have intensities of mass peaks 29, 30, 42, 46 and 75 that are more than 5-10 times that of those collected at the very next set of data points. There is also an obvious relationship between the location of the burning surface and the change in density of products sampled as the transition from gas to condensed phase occurs. At the moment the probe touches the burning surface, an abrupt change in intensities of mass peaks 2, 18, 27, 44 was not observed (for mass peaks 27 and 44 it is shown in Fig.4). It was supposed that the peaks that abruptly grew are associated with HMX. Other peaks that either did not change or decreased after the moment the probes touched the burning surface are HMX decomposition products. The ratio between the intensities of abruptly changing mass peaks in the mass-spectrum at and immediately after the moment the probe touches the burning surface is close to the ratio between the intensities of peaks in the mass-spectrum of HMX vapor obtained in [10] at an electron energy of 70 eV. However, there are some discrepancies in intensities of mass peaks 30 and 75. It is very likely that the discrepancies are associated with different experimental conditions, including the system of delivery of sampled gas to the ion source of the mass-spectrometer. The mass-spectrum of HMX vapor, obtained for our calibration at 70 eV, is presented in Table 3 (**). The intensity of mass peaks 29, 30, 42, 46, 75 coincides with those in the mass-spectrum obtained when the probe touches the propellant burning surface (*). So, we identified HMX vapor near the burning surface in HMX/GAP flame at 0.5 MPa.

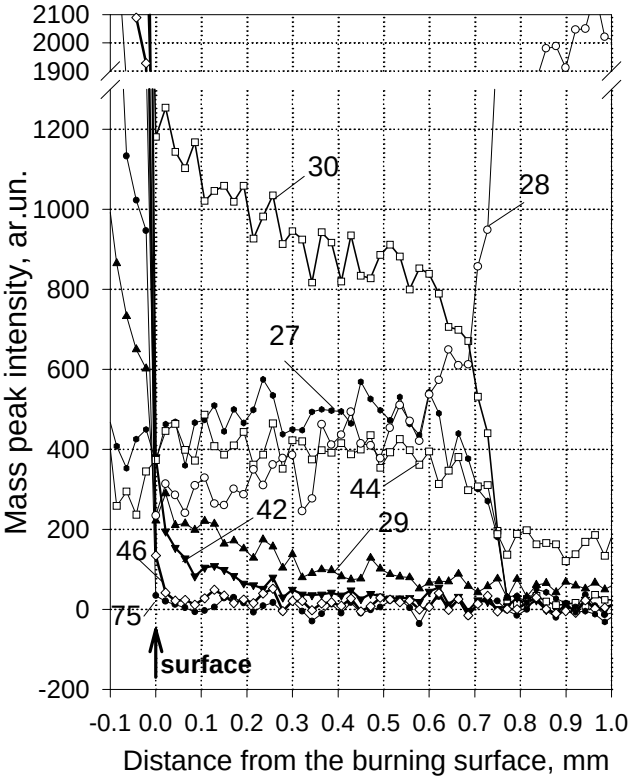


**Figure 4.** Profiles of intensities of mass peaks of combustion species in flame of $HMX_{20}$/GAP (80/20) propellant at a pressure of 0.5 MPa (Probe 1).

**Table 3**
Mass spectra of HMX vapor

| | 28 | 29 | 30 | 42 | 46 | 56 | 71 | 75 |
|---|---|---|---|---|---|---|---|---|
| HMX [10] | 38 | 14.7 | 25.5 | 100 | 65.4 | 19.2 | 9 | 51.4 |
| HMX/GAP* | 46 | 18 | 69 | 100 | 60 | 9.6 | 4.4 | 30 |
| HMX** | | 15 | 71 | 100 | 62 | | | 37 |

* - mass spectrum of the products near the burning surface of the propellant (this paper)
** - mass spectrum of the products at the HMX thermal decomposition in gas flow reactor

In addition, in the zone near the surface, mass peaks 39, 41, 42, 43 were detected. These peaks were not identified (except part of mass peak 42), but it was established that they decreased with an increase in

distance from the burning surface. We suppose that products of combustion and/or thermal decomposition of GAP are responsible for these peaks. These peaks were not taken into consideration in calculations of composition of the combustion products. The composition of combustion products (in mole fractions) of HMX/GAP propellant at a pressure of 0.5 MPa at different distances from the burning surface is presented in Table 4. The concentration of products near the burning surface (L=0 mm) obtained in 4 different experiments using Probe 1 and Probe 2 are presented in Table 4.

According to data of [2], temperature of the burning surface of HMX/GAP propellant at 0.5 MPa is equal to 603 K that is ~ 50 K higher than the melting point of HMX. Therefore HMX is already melted on the burning surface. Video recording of combustion of the propellant confirmed this statement.

Composition of products near the burning surface of HMX/GAP propellant is not reproduced from experiment to experiment. The main difference is observed in the concentration of $HMX_v$, NO, $NO_2$ and $H_2O$. The main reason for this irreproducibility is non-uniformity of the burning surface and the presence of black particles on the burning surface that were revealed by video recording. These particles slightly move on the burning surface and probably represent partially decomposed GAP. Therefore the observed irreproducibility of the composition of products near the burning surface is mainly connected with the presence or absence of "GAP particles" on the burning surface in the place under the tip of the probe. This implies that it is better to use averaged (obtained using data from several experiments (Table 4)) composition of products near the burning surface for application as a boundary condition in the combustion model of HMX/GAP propellant at 0.5 MPa.

**Table 4**

Species concentration in flame of HMX/GAP (80/20) propellant at 0.5 MPa at different distances from the burning surface (in mole fractions)

| L, mm | T, K | $H_2$ | $H_2O$ | HCN | $N_2$ | CO | NO | $CH_2O$ | $CO_2$ | $NO_2$ | $N_2O$ | $HMX_v$ |
|---|---|---|---|---|---|---|---|---|---|---|---|---|
| 0 | 603[1)] | 0.06 | 0.20 | 0.15 | 0.17 | | 0.24 | 0.05 | 0.03 | 0.03 | 0.05 | 0.01 |
| | | 0.07 | 0.17 | 0.14 | 0.17 | | 0.19 | 0.05 | 0.03 | 0.06 | 0.05 | 0.08 |
| | | 0.05 | 0.06 | 0.13 | 0.14 | | 0.10 | 0.05 | 0.02 | 0.14 | 0.04 | 0.27 |
| | | 0.04 | 0.14 | 0.13 | 0.14 | | 0.12 | 0.06 | 0.03 | 0.11 | 0.04 | 0.18 |
| 0-0.2[2)] | ~ 700 | - | 0.10 | 0.26 | 0.08 | 0.07 | 0.14 | 0.14 | 0.02 | 0.10 | 0.07 | - |
| 1.2 | 2550[3)] | 0.23 | 0.12 | 0 | 0.29 | 0.34 | 0 | 0 | 0.03 | 0 | 0 | 0 |
| Equil[4)] | 2594 | 0.225 | 0.115 | $<10^{-4}$ | 0.289 | 0.335 | $<10^{-4}$ | $<10^{-4}$ | 0.027 | $<10^{-4}$ | $<10^{-4}$ | 0 |

1) data of surface temperature of propellant from Ref. [2];
2) data of laser supported (100 $W/cm^2$) combustion of propellant at 0.1 MPa from Ref. [3];
3) corrected for heat loss by radiation;
4) equilibrium concentrations for H (0.007) and OH ($7*10^{-4}$) radicals are not presented in the table

Comparison of our data for flame structure of HMX/GAP propellant at 0.5 MPa at self-sustained combustion with data of [3] on laser supported combustion of HMX/GAP propellant at 100 $W/cm^2$ and 0.1 MPa showed that qualitatively they are similar, but differ quantitatively. It is difficult to conduct reasonable quantitative comparison of compositions of combustion products near the burning surface obtained in the present investigation and with that in [3] because of different experimental conditions. The main distinctions between our data from data in [3] are the absence of HMX vapor near the burning surface and the absence of $H_2$ in the data in [3]. The measuring system in [3] did not allow for the detection of hydrogen. The absence of HMX vapor in data [3] is probably connected with both its decomposition on the wall of the microprobe, and the insufficient spatial resolution of the sampling system used in [3], which possibly did not allow for the correct measurement of products in a narrow zone with a width of just 0.1 mm.

The composition of combustion products for HMX/GAP propellant at 0.5 MPa at a distance of 1.2 mm from the burning surface approaches a composition at thermodynamic equilibrium (Table 4, equil).

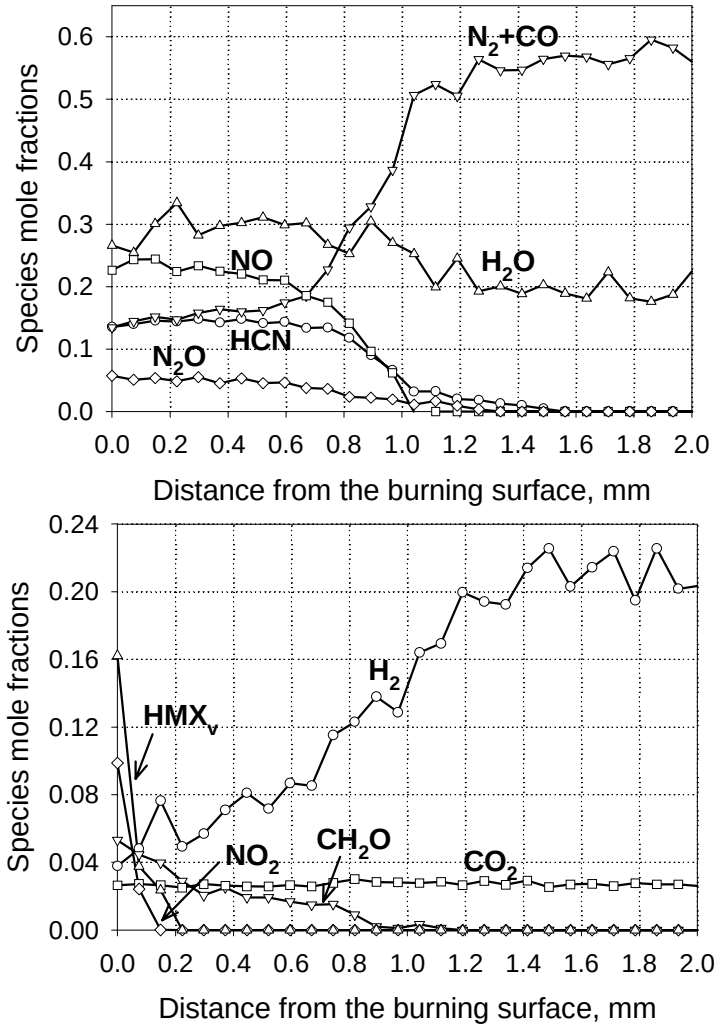


**Figure 5**. Concentration profiles in flame of HMX/GAP propellant at 0.5 MPa. (Probe 2).

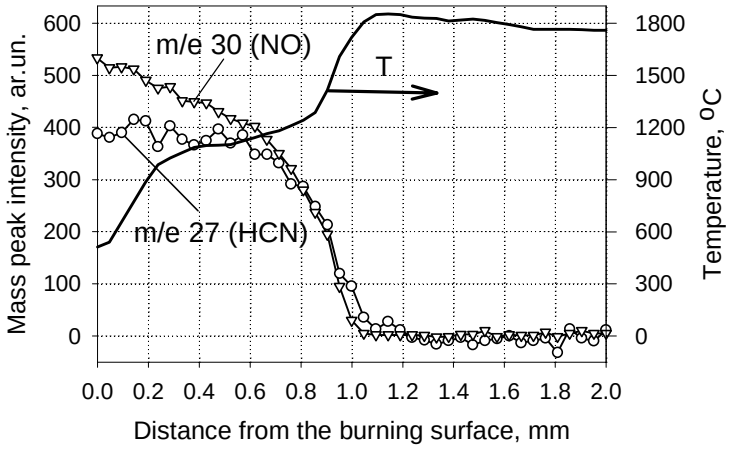


**Figure 6.** Influence of "rough" probe on flame structure of HMX/GAP propellant at a pressure of 0.5 MPa.

The flame structure of $HMX_{20}$/GAP propellant at 0.5 MPa, obtained using Probe 2, is presented in Fig. 5. Two zones of chemical reactions in the flame have been detected: 1) a narrow zone adjacent to the burning surface; 2) a luminous zone. In the first narrow zone (dark zone) near the burning surface, partial consumption of $CH_2O$ and complete consumption of $NO_2$ and HMX vapor occurs. Next, the induction zone is observed in the concentration profiles (at a distance of 0.2-0.7 mm from the burning surface) where insignificant consumption of $N_2O$ and $CH_2O$ with formation of $H_2$, CO and $N_2$ occurs, and concentrations of all the rest of the products remain essentially constant. In the second zone (luminous), at a distance of 0.7-1.0 mm from the burning surface, abrupt consumption of NO, HCN, $CH_2O$ and $N_2O$ with formation of $H_2$, $N_2$ and CO takes place. The width of consumption zone of HCN (~ 1.6 mm) is significantly larger than that of other products (~ 1 mm for NO and $CH_2O$). Comparison of species concentration profiles (Fig.5) with measured temperature profiles (Fig.3) shows that they have different characteristics. The latter show an almost constant, monotonic increase of temperature. Whereas Fig.5 shows that there is a wide region (0.2-0.6 mm) where concentrations of almost all species remains essentially constant. In order to establish an explanation for this discrepancy, experiments with simultaneous measurement of concentration profiles of species and temperature profile in the regions probed were conducted. A thermocouple was located at a distance of 0.35 mm from the tip of the probe. The "roughest" probe (Probe 1) was chosen for these experiments. Temperature was measured using a flat WRe(5%)- WRe(20%) thermocouple with a thickness of 12 μm. Profiles of the most characteristic mass peaks (with m/e=27 (HCN) and m/e=30 (NO)) and temperature are presented in Fig. 6. It is evident that the concentration and temperature profiles are similar. Thus, thermal perturbation of the flame by the probe accounts for the presence of the induction zone in the concentration profiles of HMX/GAP propellant flame at 0.5 MPa in

the results of experiments shown in Fig. 5 and Fig. 6. Video recording revealed that the width of the dark zone of the HMX/GAP flame at 0.5 MPa is ~ 0.4 mm (without probe), and increases to 0.7-0.8 mm, when the "rough" probe (Probe 1 or Probe 2) is used.

Fig. 7 shows profiles of intensities of mass peaks with m/e=27 (HCN) and m/e=30 (NO) in a HMX/GAP flame at 0.5 MPa, obtained using Probe 3, and the temperature profile (Fig.3) of an unperturbed flame. It is obvious that the profiles are similar. Profiles of intensities of mass peaks with m/e=44 ($CO_2$, $N_2O$), m/e=28 ($N_2$, CO), m/e=29 ($CH_2O$), m/e=2 ($H_2$), m/e=17 (fragmentary peak of $H_2O$) were also measured. However in this experiment we could not separate contributions of species with the same molecular weight using peaks of fragmentary ions, as was done earlier, because available time of this experiment with Probe 3 was ≤0.6 s. Profiles of the intensities of the mass peaks that are most characteristic and most intense in the HMX/GAP flame at 0.5 MPa (see Fig. 5) are presented in Fig. 7. The induction zone in the concentration profiles of HCN and NO that was detected in experiments with Probe 1 (Fig.6) and Probe 2 (Fig.5) was not observed with Probe 3. Concentrations of these species decreased continuously, beginning from the burning surface. The width of the consumption zone of NO is ~ 0.65 mm, and of HCN ~ 1.0 mm. Video recording shows that the width of the dark zone did not change as Probe 3 approached the burning surface.

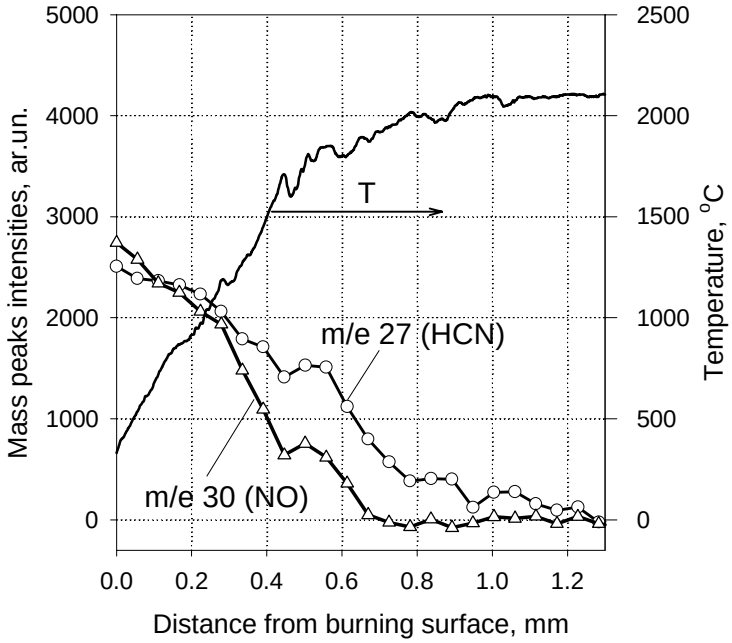


**Figure 7**. Profiles of intensities of mass peaks with m/e=27 (HCN) and m/e=30 (NO) in HMX/GAP flame at 0.5 MPa (Probe 3).

## 4. CONCLUSIONS

- Chemical and thermal structure of the flame of an HMX/GAP (80/20) propellant has been investigated at a pressure of 0.5 MPa by molecular beam mass spectrometry method using an advanced probing technique, microthermocouples and video recording.
- Eleven species, including HMX vapor, have been detected in the zone adjacent to the burning surface. Species concentrations have been determined at different distances from the burning surface.
- Comparison of flame structure at self-sustained combustion of HMX/GAP propellant at 0.5 MPa with data from laser supported combustion of the same propellant at 0.1 MPa showed that qualitatively they are similar, but that they differ quantitatively.
- Temperature profiles in the combustion wave have been measured and compared with data of other researchers. The difference between those sets of data most likely relates to different types of GAP used in the propellants**.**
- Two zones of chemical reactions in the flame have been detected: 1) a narrow zone adjacent to the burning surface; 2) a luminous zone. In the first narrow zone near the burning surface, partial consumption of $CH_2O$ and complete consumption of $NO_2$ and HMX vapor occur. In the second zone, consumption of NO, HCN, $CH_2O$ and $N_2O$ with formation of $H_2$, $N_2$ and CO takes place. The width of consumption zone of NO is of ~ 0.65, and of HCN is ~1.0 mm.
- The data obtained can be used for creation and validation of a combustion model for propellants based on HMX and GAP.

## ACKNOWLEDGMENT

This research is supported by US Army Research Office under grant #DAAD19-02-1-0373. The assistance of Dr. Rose Ann Pesce-Rodriguez with the English editing of the paper is gratefully acknowledged.

## REFERENCES

1. N. Kubota, and T. Sonobe, "Burning Rate Catalysis of Azide/Nitramine Propellants," Proceedings of Twenty-third Symposium (International) on Combustion, Combustion Inst., Pittsburgh, PA, 1990, pp. 1331-1337.
2. A.A. Zenin, and S.V. Finjakov, "Physics of Combustion of Energetic Binder-Nitramine Mixtures," Proceedings of the 33rd International Annual Conference of ICT, Fraunhofer Institut Chemische Technologie, Karlsruhe, 2002.
3. T.A. Litzinger, Y. Lee, C-J. Tang, "Experimental Studies of Nitramine/Azide Propellant Combustion," Solid Propellant Chemistry, Combustion, and Motor Interior Ballistics, edited by V. Yang, T.B. Brill, and W.-Z. Ren, Vol. 185, Progress in Astronautics and Aeronautics, AIAA, Reston, VA, 2000, pp. 355-379.
4. E.S. Kim, V. Yang, Y.-C. Liau, "Modeling of HMX/GAP Pseudo-Propellant Combustion", Combustion and Flame, 131:227-245, 2002.
5. O.P. Korobeinichev, "Flame Structure of Solid Propellants" Solid Propellant Chemistry, Combustion, and Motor Interior Ballistics, edited by Vigor Yang, Thomas B. Brill, and Wu-Zhen Ren.Vol. 185, Progress in Astronautics and Aeronautics, AIAA, New York , 2000, pp.335-354.
6. J.L. Lyman, Y.-C. Liau, H.V. Brand, "Thermochemical Function for Gas-Phase, 1,3,5,7,-Tetranitro-1,3,5,7-tetraazacyclooctane (HMX), Its Condensed Phases, and Its Larger Reaction Products", Combustion and Flame 130:185-203 (2002).
7. A.A. Zenin, "Experimental Investigation of the Burning Mechanism of Solid Propellants and Movement of Burning Products", Ph.D. Dissertation, Inst. of Chemical Physics, USSR Academy of Sciences, Moscow, USSR, 1976 (in Russian).
8. A.G. Tereshenko, O.P. Korobeinichev, A.A. Paletsky, L.T. DeLuca, "Laser-Supported Ignition, Combustion and Gasification of AP-based Propellants", Proceedings of The 8th International Workshop on Combustion and Propulsion, Pozzuoli, Naples, Italy, 16-20 June, 2002, paper 24(1-10).
9. Korobeinichev, O.P., Kuibida, L.V., Paletsky, A.A., and Shmakov, A.G., "Molecular-Beam Mass-Spectrometry to Ammonium Dinitramide Combustion Chemistry Studies," *Journal of Propulsion and Power*, Vol. 14, No. 6, 1998, pp. 991-1000.
10. R. Behrens, Jr., "Identification of Octahydro-1,3,5,7-tetranitro-1,3,5,7-tetrazocine (HMX) Pyrolysis Products by Simultaneous Thermogravimetric Modulated Beam Mass Spectrometry and Time-of-Flight Velocity-Spectra Measurements", International Journal of Chemical Kinetics, vol. 22, 1990, pp. 135-157.
11. Korobeinichev, O.P., Kuibida, L.V., Madirbaev, V. Zh., "Investigation of the Chemical Structure of the HMX Flame", Combustion, Explosion and Shock Waves, Vol. 20, No. 3, 1984, pp. 282-285.